

---

## WIRE ELECTRICAL DISCHARGE MACHINING OF A HYBRID COMPOSITE: EVALUATION OF KERF WIDTH AND SURFACE ROUGHNESS

*Abdil KUŞ\**  
*Ali Rıza MOTORCU\*\**  
*Ergün EKİCİ\*\**

---

Received: 12.06.2015, revised: 12.05.2016, accepted: 17.06.2016

**Abstract:** In this study, the machinability characteristics of Al/B4C-Gr hybrid composite were investigated using wire electrical discharge machining (WEDM). In the experiments, the machining parameters of wire speed, pulse-on time and pulse-off time were varied in order to explain their effects on machining performance, including the width of slit (kerf) and surface roughness values (Rz and Rt). According to the Taguchi quality design concept, a L18 (21×32) orthogonal array was used to determine the S/N ratio, and analysis of variance (ANOVA) and the F-test were used to indicate the significant machining parameters affecting the machining performance. From the ANOVA and F-test results, the significant factors were determined for each of the machining performance criteria of kerf, Rz and Rt. The variations of kerf, Rz and Rt with the machining parameters were statistically modeled via the regression analysis method. The optimum levels of the control factors for kerf, Rz and Rt were specified as A1B1C1, A1B1C2 and A1B1C2, respectively. The correlation coefficients of the predictive equations developed for kerf, Rz and Rt were calculated as 0.98, 0.828 and 0.855, respectively.

**Keywords:** Wire EDM, kerf, surface roughness, hybrid composite, Taguchi method

### **Karma Kompozitin Tel Elektro Erozyon Tezgâhında İşlenmesinde: Kesim Genişliği ve Yüzey Pürüzlülüğünün Değerlendirilmesi**

**Öz:** Bu çalışmada, Al/B4C-Gr karma kompozitin tel elektro erozyon tezgâhında işlenebilirlik karakteristikleri araştırılmıştır. Deneylerde; kesim genişliği (kerf) ve yüzey pürüzlülük değerlerini (Rz ve Rt) içeren işleme performansı etkilerinin incelenmesinde tel hızı, vuruş süresi ve vuruş ara süresi işleme parametreleri olarak seçilmiştir. Taguchi kalite tasarım konseptine göre, S/N oranını tanımlamak için bir L18 (21×37) ortogonal dizi ve işleme performansını etkileyen anlamlı işleme parametrelerini belirlemek için varyans analizi (ANOVA) ve F-testi kullanılmıştır. ANOVA ve F-testi sonuçlarından, işleme performansı kriterleri kerf, Rz ve Rt'nin her biri için anlamlı faktörler belirlendi. İşleme parametreleri ile kerf, Rz ve Rt'nin değişimleri regresyon analizi metodu yardımıyla istatistiksel olarak modellenmiştir. Kerf, Rz ve Rt için kontrol faktörlerinin optimum seviyeleri sırasıyla A1B1C1, A1B1C2 ve A1B1C2

---

\* Uludağ University, Mechanical Program, Technical Sciences Vocational School, Bursa

\*\* Çanakkale Onsekiz Mart University, Faculty of Engineering, Dept. of Industrial Engineering, Çanakkale

Corresponding Author: Abdil KUŞ (abdilkus@uludag.edu.tr)

olarak belirlendi. Kerf, Rz ve Rt için geliştirilen tahminsel denklemlerin korelasyon katsayıları sırasıyla 0.98, 0.828 ve 0.855 olarak hesaplanmıştır.

**Anahtar kelimeler:** Tel elektro erozyon, kesim genişliği, yüzey pürüzlülüğü, karma kompozit, Taguchi metot

## 1. INTRODUCTION

Metal matrix composites (MMCs) are widely preferred in today's engineering applications due to their characteristics of high strength, lightness, wear resistance and thermal stability (Krishnamurthy et al., 2007, Ravikiran et al., 1197 and Lin et al., 2009). However, because of the highly abrasive characteristics of their reinforcement elements, such as  $Al_2O_3$ , SiC and  $B_4C$ , using conventional methods in the machining of MMCs is relatively difficult (Kevin et al., 2005, Iwai et al., 2000, Hu et al., 2001 and Çifçi et al., 2004). In order to overcome this problem, non-conventional machining processes such as electrical discharge machining (EDM), laser beam machining (LBM), abrasive water jet (AWJ) machining and wire electrical discharge machining (WEDM) offer effective alternatives (Puhan et al., 2013). However, LBM and AWJ are not desirable applications because of the high cost and poor quality of the resulting workpiece surface (Lau et al., 1995). At this stage, EDM and WEDM become promising options, and WEDM is seen as an economical and effective application for unproblematic machining of MMCs with complex geometries (Garg et al., 2010). Wire EDM is a thermo-electrical process used to remove material from the workpiece by means of a series of sparks created between the workpiece and an electrode immersed in a liquid dielectrical medium (Singh and Garg, 2011). There is no contact between the electrode and the workpiece and, while electrical conductivity is important for the materials to be machined, the hardness of the workpiece is not a limiting factor (Lahane et al., 2012). The most important performance measurements in WEDM are the material removal rate (MRR), or cutting speed, workpiece surface finish and kerf (cutting width or width of slit). Kerf specifies the dimensional accuracy of the machined part (Saha et al., 2013). Discharge current, discharge capacitance, pulse duration, pulse frequency, wire speed, wire tension, average working voltage and dielectric flushing conditions are known to be the machining parameters, which affect the performance measurements (Tosun et al., 2004). In other studies, researchers have investigated the effects of machining parameters on WEDM performance. For example, Lauwers et al. examined the effects of electrical conductive phase type and particle size of  $ZrO_2$  ceramic composites on WEDM performance (Lauwers et al., 2008). Fard et al. evaluated the machining of Al-SiC composites in dry WEDM via intelligent modeling and multi-characteristics optimization (Fard et al., 2013). Shandilya et al. using response surface methodology (RSM) and an artificial neural network (ANN) evaluated the average cutting speed of SiCp/6061 Al MMCs in WEDM (Shandilya et al., 2013). Prakash et al. investigated the machinability of (A413)/Flyash/ $B_4C$  hybrid composites (produced by the stir casting method) in WEDM via the Taguchi method (TM) (Prakash et al., 2013). Muthuraman and Ramakrishna studied the machinability of WC-Co composites by multi-parametric optimization (Muthuraman and Ramakrishna, 2012). The machinability of Al/SiC MMCs in the CNC wire cut EDM was examined by Manna and Bhattacharyya by using the TM and Gauss elimination method (Manna and Bhattacharyya, 2006). Rozenek et al. carried out studies on the effect of machining parameters (discharge current, pulse-on time, pulse-off time, voltage) on machining feed rate and surface roughness in the WEDM of AlSi7Mg/SiC and AlSi7Mg/ $Al_2O_3$  MMCs (Rozenek et al., 2001). Saha et al., used soft computing models for the estimation of the surface roughness and cutting speed of tungsten carbide cobalt composites in WEDM (Saha et al., 2008). The effects of the machining parameters and  $Al_2O_3$  reinforcement ratio of  $Al_2O_3$ p/6061Al composites on the cutting speed (MMR), surface roughness and width of slit in WEDM were investigated by Yan et al., 2005.

Patil and Brahmanekar, used dimensional analysis in the evaluation of the MMR of Al/SiCp composites in WEDM depending on the SiC reinforcement ratio (Patil and Brahmanekar, 2010a). Satishkumar et al., studied the effects of the pulse-on time, pulse-off time, gap voltage, wire speed and wire feed parameters of Al6063/SiC on MRR and surface roughness ( $Ra$ ) in WEDM (Satishkumar et al., 2011). In another study by Patil and Brahmanekar, the TM was used to evaluate the effects of reinforcement, current, pulse-on time, pulse-off time, servo reference voltage and the maximum feed speed, wire speed, flushing pressure and wire tension of Al/Al<sub>2</sub>O<sub>3</sub> composites on the cutting speed, surface finish, and kerf width in WEDM (Patil and Brahmanekar, 2010b).

The present study used the Taguchi method to investigate the effects of the control factors of wire speed ( $WS$ ), pulse-on time ( $T_{on}$ ) and pulse-off time ( $T_{off}$ ) on kerf ( $K$ ) and surface roughness ( $R_z$  and  $R_t$ ) in the cutting of Al/B<sub>4</sub>C-Gr MMCs with WEDM. As a result, the effects of control factors in the use of WEDM for the machining of B<sub>4</sub>C-Gr hybrid composites in particular were determined, thus compensating for the lack of coverage in the literature.

## 2. MATERIALS AND METHODS

In the production of Al/B<sub>4</sub>C-Gr hybrid composites, 200 μm submicron Alumix 123 alloy was used as the matrix element, and an average of 27 μm B<sub>4</sub>C and -150 μm Gr particles were used as the reinforcement elements. The hybrid composites were produced by cold pressing less than 100 MPa pressure and then by hot pressing at 590 °C for 15 min under 40 MPa pressure. The samples thus produced were solution treated at 540 °C for 4 h, immersed in warm water (25 °C), and then subjected to T6 heat treatment by holding them in the furnace at 160 °C for 12 h. The tests were made with a Sodick AQ750LH CNC Wire EDM machine. A copper electrode of 0.25 mm in diameter was employed as the cutting tool and 20 °C deionized water was used as the dielectric liquid. For the surface roughness measurements, depending on the specified control factors, 6 mm-long cuttings were made with respect to the test conditions in Table 2. For the kerf ( $K$ ) measurements, in addition to the surface roughness cuttings, 3 mm-long cuttings were made and at the end, the wire was broken off in order to prevent the workpiece from being cut in two. The Time TR 200 portable surface roughness instrument, seen in Fig. 1, was used for the surface roughness measurements, which were made perpendicular to the wire feed direction at a cut-off length of 4 mm. The arithmetic mean of the measurements taken from five different areas of the cut surface was used. Kerf measurements were made by a Dino Capture 2.0 optical microscope and the arithmetic mean of measurements taken from five different points was used (Fig. 2).



**Figure 1:**  
*Portable surface roughness measurement device used at the measurements.*

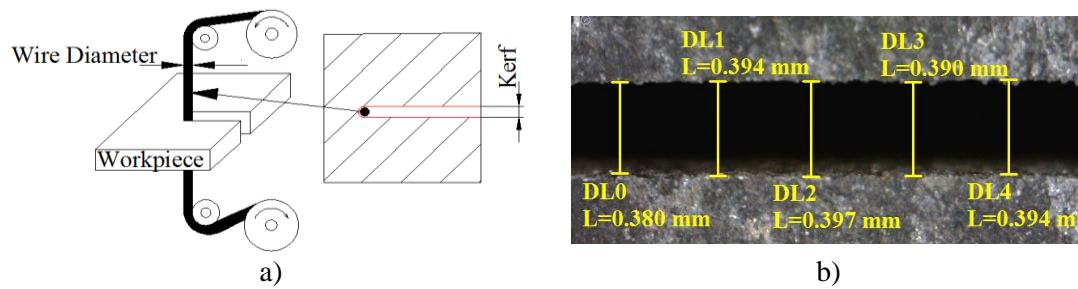


**Figure 2:**  
Definition of the kerf and its measurement on the workpiece after cutting in the WEDM

Arithmetical mean roughness ( $R_a$ ) does not give any information about the surface roughness wavelength and is not sensitive to the small variations in the profile. Therefore, in this study, both the  $R_z$  (ten-point mean roughness) and the  $R_t$  (maximum roughness height) measurement results were taken into consideration. The  $R_z$  is more sensitive than the  $R_a$  because it can better express high peaks and deep valleys. The International Organization for Standardization (ISO) system defines this parameter ( $R_z$ ) as the height difference of the average of the highest five peaks and lowest five valleys throughout the profile evaluation. The  $R_t$  is defined as the vertical distance between the highest peak and the lowest valley throughout the cut-off length. The  $R_t$  is very sensitive as it expresses the high peaks or deep valleys.

The kerf ( $K$ , mm) and surface roughnesses ( $R_z$ ,  $R_t$ ,  $\mu\text{m}$ ) of  $\text{AlB}_4\text{C-Gr}$  hybrid composites in WEDM were investigated. Wire speed ( $WS$ ), pulse-on time ( $T_{on}$ ) and pulse-off time ( $T_{off}$ ) were selected as the machining parameters (control factors). These control factors and their levels are given in Table 1.

**Table 1. Control factors and their levels.**

Symbol	Control Factors	Unit	Level		
			1	2	3
A	Wire speed	(m/min)	-	50	70
B	Pulse-on time	( $\mu\text{s}$ )	5	7	10
C	Pulse-off time	( $\mu\text{s}$ )	7	10	14

### 3. EXPERIMENTAL DESIGN VIA THE TAGUCHI METHOD

Taguchi experimental design uses orthogonal arrays extensively and is an efficient tool for improving process/product quality with a relatively fewer number of experimental runs (Puhan et al., 2013). Taguchi experimental design is used to provide information such as control, main and interaction factor effects by carrying out a minimum number of tests.

The purpose of the Taguchi method (TM) is to find the best combination of design parameters with minimum variation (Rubio et al., 2013). Test results are then converted to a signal to noise (S/N) ratio. The S/N ratio is used to identify and measure the deviation of the quality characteristics from the required values (Vankanti and Ganta, 2014). The S/N ratios are calculated with respect to “smaller the better” (SB), “nominal the best” (NB) and “higher the better” (HB) approaches (Ross, 1996). In the determination of  $K$ ,  $R_z$  and  $R_t$ , the SB approach (Eq. 1) was used.

Smaller the better:

$$S / N_{SB} = -10 \log \left( \frac{1}{n} \sum_{i=1}^n y_i^2 \right) \quad (1)$$

In this study, for the determination of the effects of the control factors on  $K$ ,  $R_z$  and  $R_t$ , the Taguchi  $L_{18}$  ( $2^1 \times 3^2$ ) orthogonal array (OA) was used. Eighteen test combinations were made depending on the selected OA and the S/N ratios of the control factors on  $K$ ,  $R_z$  and  $R_t$  (Table 2).

**Table 2. L18 ( $2^1 \times 3^2$ ) orthogonal array, experimental results and their S/N ratios**

Exp. no	Designation	Control factors			Observed values			S/N ratio (dB)		
		A	B	C	$K$ [mm]	$R_z$ [ $\mu\text{m}$ ]	$R_t$ [ $\mu\text{m}$ ]	$K$	$R_z$	$R_t$
1	A <sub>1</sub> B <sub>1</sub> C <sub>1</sub>	50	5	7	0.398	18.45	23.44	8.00	-25.32	-27.40
2	A <sub>1</sub> B <sub>1</sub> C <sub>2</sub>	50	5	10	0.406	16.45	24.05	7.83	-24.32	-27.62
3	A <sub>1</sub> B <sub>1</sub> C <sub>3</sub>	50	5	14	0.409	16.88	21.87	7.77	-24.55	-26.80
4	A <sub>1</sub> B <sub>2</sub> C <sub>1</sub>	50	7	7	0.413	21.59	28.07	7.68	-26.69	-28.96
5	A <sub>1</sub> B <sub>2</sub> C <sub>2</sub>	50	7	10	0.417	20.17	28.12	7.60	-26.09	-28.98
6	A <sub>1</sub> B <sub>2</sub> C <sub>3</sub>	50	7	14	0.424	19.45	25.02	7.45	-25.78	-27.97
7	A <sub>1</sub> B <sub>3</sub> C <sub>1</sub>	50	10	7	0.419	18.82	24.28	7.56	-25.49	-27.70
8	A <sub>1</sub> B <sub>3</sub> C <sub>2</sub>	50	10	10	0.424	18.21	21.00	7.45	-25.21	-26.44
9	A <sub>1</sub> B <sub>3</sub> C <sub>3</sub>	50	10	14	0.434	19.32	24.13	7.25	-25.72	-27.65
10	A <sub>2</sub> B <sub>1</sub> C <sub>1</sub>	70	5	7	0.399	17.74	21.57	7.98	-24.98	-26.68
11	A <sub>2</sub> B <sub>1</sub> C <sub>2</sub>	70	5	10	0.406	17.78	20.60	7.83	-25.00	-26.28
12	A <sub>2</sub> B <sub>1</sub> C <sub>3</sub>	70	5	14	0.409	19.90	23.12	7.77	-25.98	-27.28
13	A <sub>2</sub> B <sub>2</sub> C <sub>1</sub>	70	7	7	0.425	20.54	24.31	7.43	-26.25	-27.72
14	A <sub>2</sub> B <sub>2</sub> C <sub>2</sub>	70	7	10	0.426	18.70	24.50	7.41	-25.44	-27.78
15	A <sub>2</sub> B <sub>2</sub> C <sub>3</sub>	70	7	14	0.434	21.74	29.73	7.25	-26.75	-29.46
16	A <sub>2</sub> B <sub>3</sub> C <sub>1</sub>	70	10	7	0.438	20.68	27.02	7.17	-26.31	-28.63
17	A <sub>2</sub> B <sub>3</sub> C <sub>2</sub>	70	10	10	0.438	22.40	28.50	7.17	-27.00	-29.10
18	A <sub>2</sub> B <sub>3</sub> C <sub>3</sub>	70	10	14	0.441	22.78	31.86	7.11	-27.15	-30.06

$T_K$ , (Kerf total mean value) = 0.420 mm.  $T_{K,S/N}$ , (Kerf S/N ratio total mean value) = 7.54 dB.

$T_{Rz}$ , ( $R_z$  surface roughness total mean value) = 19.534  $\mu\text{m}$ .  $T_{Rz,S/N}$ , ( $R_z$  surface roughness S/N ratio total mean value) = -25.78 dB.

$T_{Rt}$ , ( $R_t$  surface roughness total mean value) = 25.066  $\mu\text{m}$ .  $T_{Rt,S/N}$ , ( $R_t$  surface roughness S/N ratio total mean value) = -27.92 dB.

Standard deviation of kerf=0.0137, Standard deviation of  $R_z$  surface roughness=1.843, Standard deviation of  $R_z$  surface roughness=3.168

## 4. RESULTS AND DISCUSSION

The results of the average measurements of  $K$ ,  $R_z$  and  $R$  obtained in the cutting of Al/B<sub>4</sub>C-Gr hybrid composites with CNC WEDM were analyzed using the Minitab 16.1 software program.

### 4.1. Analysis and optimization of the performance characteristics

The averages of test measurement results and S/N ratios are shown in Table 3. The highest S/N ratio in the factor levels represents the best performance (minimum  $K$ ,  $R_z$  and  $R_t$ ). The

average S/N ratios for  $K$ ,  $R_z$  and  $R_t$  were calculated as 7.54 dB, -25.78 dB and -27.92dB, respectively. Higher and lower differences between the highest and the lowest S/N ratios calculated at different levels of each of the control factors were used for the determination of effective factors on  $K$ ,  $R_z$  and  $R_t$  (31.Durairaja et al., 2013). As seen from Table 3, the effective factors on  $K$  were pulse-on time (B), pulse-off time (C) and wire speed (A). The effective factors on  $R_z$  and  $R_t$  were pulse-on time (B), wire speed (A) and pulse-off time (C). The optimum S/N ratios of the control factors are given in Table 4. Here, the optimum levels of the control factors  $K$ ,  $R_z$  and  $R_t$  were  $(A_1B_1C_1)$ ,  $(A_1B_1C_2)$  and  $(A_1B_1C_2)$ , respectively. It was observed that the most effective parameter on the performance characteristics was pulse-on time (B).

**Table 3. Response table for means of  $K$ ,  $R_z$  and  $R_t$**

Level	$K$ [mm]			$R_z$ [ $\mu$ m]			$R_t$ [ $\mu$ m]		
	A	B	C	A	B	C	A	B	C
1	<b>0.4160*</b>	<b>0.4045*</b>	<b>0.4153*</b>	<b>18.82</b>	<b>17.87*</b>	19.64	<b>24.44</b>	<b>22.44*</b>	24.78
2	0.4240	0.4232	0.4195	20.25	20.36	<b>18.95*</b>	25.69	26.62	<b>24.46*</b>
3	-	0.4323	0.4252	-	20.37	20.01	-	26.13	25.96
$\Delta$	0.0080	0.0278	0.0098	1.44	2.50	1.06	1.25	4.18	1.49
Rank	3	1	2	2	1	3	3	1	2

\*Optimum level,  $\Delta$ = difference between maximum and minimum.

**Table 4. S/N response table for  $K$ ,  $R_z$  and  $R_t$**

Level	$K$ [mm]			$R_z$ [ $\mu$ m]			$R_t$ [ $\mu$ m]		
	A	B	C	A	B	C	A	B	C
1	7.621	7.862	7.637	-25.46	-25.02	-25.84	-27.73	-27.01	-27.85
2	7.458	7.471	7.549	-26.10	-26.17	-25.51	-28.11	-28.48	-27.70
3	-	7.285	7.433	-	-26.15	-25.99	-	-28.27	-28.20
$\Delta$	0.163	0.577	0.204	0.63	1.14	0.48	0.38	1.47	0.50
Rank	3	1	2	2	1	3	3	1	2

$\Delta$ = difference between maximum and minimum.

**4.2. The effects of control factors on the performance characteristics**

The performance characteristics of the control factors of Al/B<sub>4</sub>C-Gr hybrid composites, i.e., wire speed ( $Ws$ ), pulse-on time ( $T_{on}$ ) and pulse-off time ( $T_{off}$ ), in cutting by WEDM and their main effects on the  $K$ ,  $R_z$  and  $R_t$  were demonstrated (Fig. 3) by using a graphical representation of the factor effects and then evaluated (Montgomery, 1991). The main effect graphics of the control factors for  $K$  are given in Fig. 3a, where  $K$  increased depending on the increasing values of the control factors. From the same graphic, it can be seen that the most effective control factor on  $K$  was pulse-on time (B) and the optimum levels  $(A_1B_1C_1)$  of the control factors were  $A_1$  ( $Ws = 50$  m/min),  $B_1$  ( $T_{on} = 5$   $\mu$ s) and  $C_1$  ( $T_{off} = 7$   $\mu$ s). In Fig. 3b and 3c, when the effects of the control factors on  $R_z$  and  $R_t$  were examined, an increase in  $R_z$  and  $R_t$  was observed, depending on the increase of wire speed. With the increase of  $T_{on}$  from 5  $\mu$ s to 7  $\mu$ s, the surface roughness of the workpiece deteriorated, but with a further increase of the  $T_{on}$  value ( $T_{on} = 10$   $\mu$ s), the roughness of the cut surface decreased (Fig. 3c). In order to obtain minimum  $R_z$  and  $R_t$  surface roughness, the optimum levels of the control factors were  $A_1$  ( $Ws = 50$  m/min),  $B_1$  ( $T_{on} = 5$   $\mu$ s) and  $C_2$  ( $T_{off} = 10$   $\mu$ s). The most effective parameter on  $R_z$  and  $R_t$  was again  $T_{on}$  (Fig. 3b and 3c).

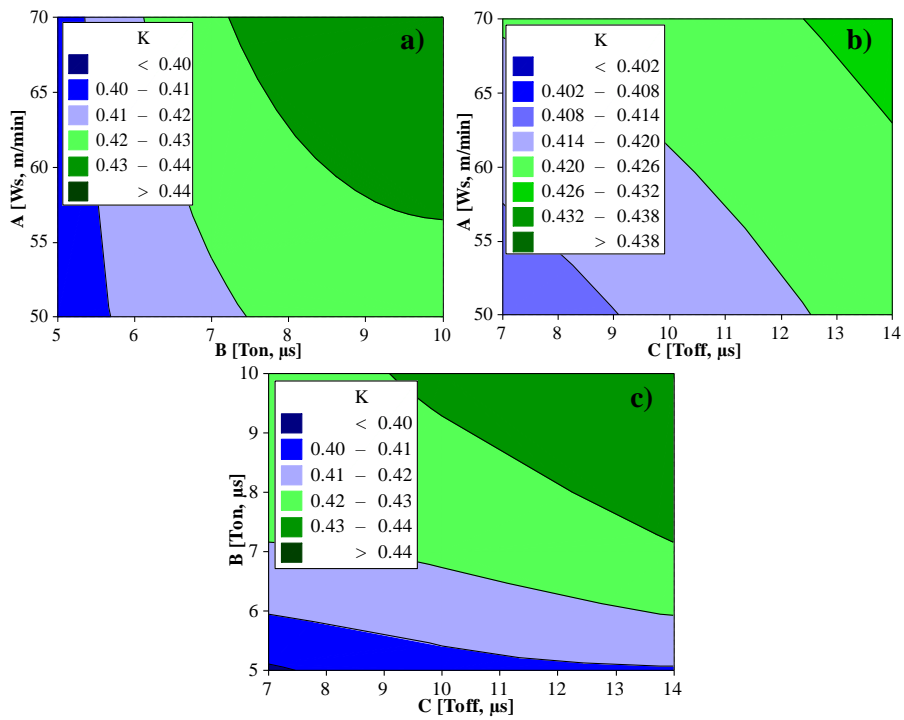


**Figure 4:**  
 Contour plots of kerf vs control factors a)  $Ws * T_{on}$  (AxB), b)  $Ws * T_{off}$  (AxC), c)  $T_{on} * T_{off}$  (BxC)

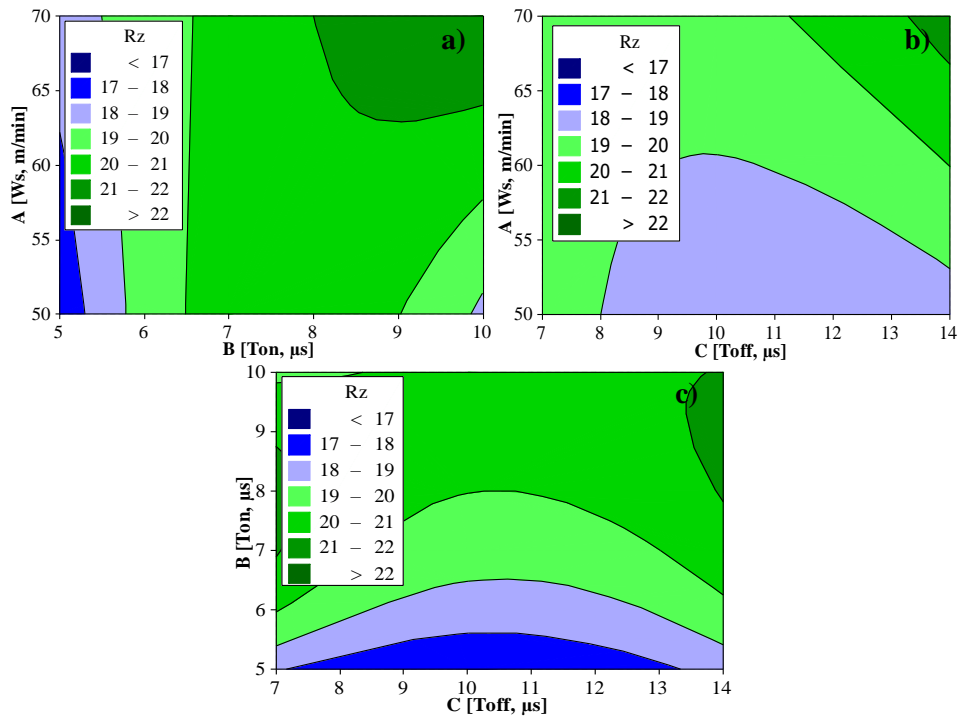


**Figure 5:**  
 Contour plots of  $R_z$  surface roughness vs control factors a)  $Ws * T_{on}$  (AxB), b)  $Ws * T_{off}$  (AxC), c)  $T_{on} * T_{off}$  (BxC)

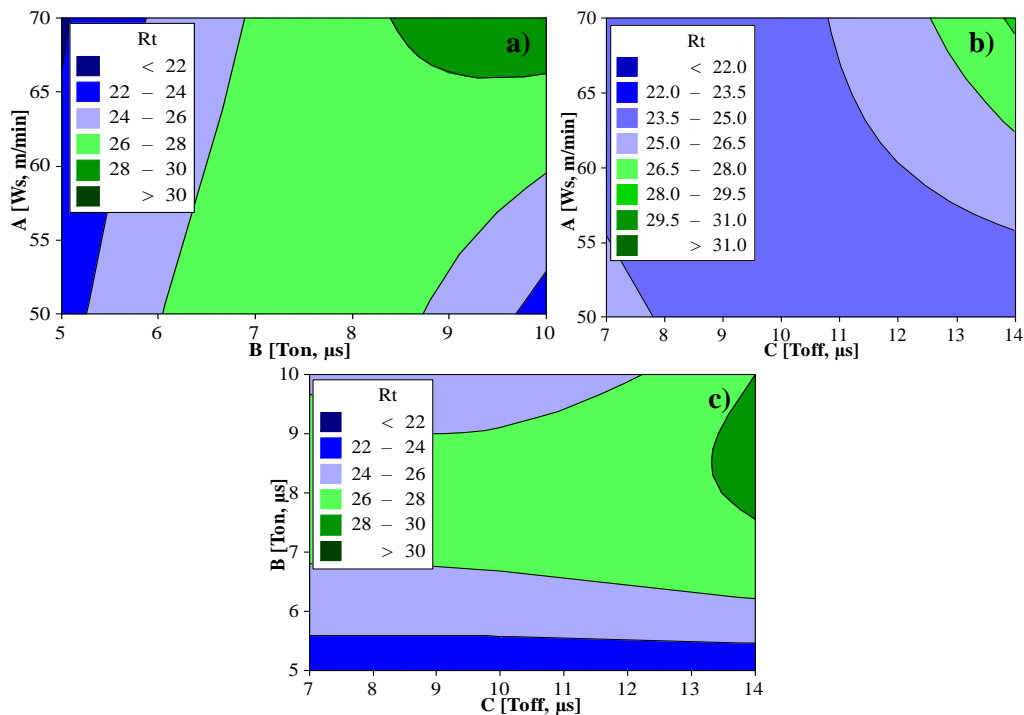


**Figure 6:**  
 Contour plots of  $R_t$  surface roughness vs control factors a)  $W_s * T_{on}$  (AxB), b)  $W_s * T_{off}$  (AxC),  
 c)  $T_{on} * T_{off}$  (BxC)

In the contour graphics (Fig. 4 and Fig. 6), variations of K, Rz and  $R_t$  are seen, depending on interactions of the control factors of wire speed, pulse-on time and pulse-off time. Fig. 4a shows that at  $T_{on}$  5  $\mu s$ , a lower value of K was obtained and the increase of wire speed did not increase K, and at  $T_{on}$  7-10  $\mu s$  and  $W_s$  58-70 m/min, the maximum K was obtained. This was explained by Yan et al., with the coefficient of thermal conductivity of the composite and can be attributed to the amount of material melting per time unit (Yan et al., 2005). When the effect of the interaction of wire speed and pulse-off time on K is examined, it can be observed that K decreased with lower wire speed and pulse-off time and increased depending on wire speed and pulse-off time (Fig. 4b). From the color changes of the two-dimensional surfaces (Fig. 4c) it is seen that pulse-on time was more effective on K than pulse-off time and K increased depending on the increase of pulse-on time; the minimum K values were obtained at  $T_{on}$  5-10  $\mu s$ . The effects of wire speed\*pulse-on time, wire speed\*pulse-off time and pulse-on time\*pulse-off time interactions on Rz are given in Figures 5a-c. The effect of wire speed\*pulse-on time interaction on Rz was similar to that on K. The Rz increased depending on the increase of wire speed and pulse-on-time (Fig. 5a). When the wire speed\*pulse-off time interaction was evaluated, a lower Rz was obtained at a lower wire speed and at  $T_{off}$  8-14  $\mu s$  (Fig. 5b). Fig. 5c shows that pulse-off time had no significant effect on Rz; the lowest Rz was obtained at the lowest pulse-on time ( $T_{on}$  5  $\mu s$ ) and at  $T_{off}$  7-13  $\mu s$ . In Figures 6a and 6c it can be seen that the effects of wire speed\*pulse-on time and pulse-on time\*pulse-off time interactions on  $R_t$  were similar to those on Rz. When the contour plot showing the effect of wire speed\*pulse-off time interaction on  $R_t$  is examined, it is seen that  $R_t$  also increased depending on the increasing wire speed and that the pulse-off time was different from that of Rz (Fig. 6b).



### 4.3. Analysis of variance (ANOVA)

Analysis of variance (ANOVA) is a statistical-based, objective decision-making tool used for determining any difference in the average performance of a group of items tested (Durairaja et al., 2013). In a case where the F value of a process parameter is greater than the tabulated F ratio, it shows that that the control factor has a significant effect on the performance characteristic. The variance analysis results expressing the effects of each process parameter on  $K$ ,  $R_z$  and  $R_t$ , depending on the F value and percentage contribution, are given in Tables 5-7. The most effective process parameter on the performance characteristic  $K$  is pulse-on time (B,  $T_{on}$ ) with a 75.13% percentage contribution (Table 5). Wire speed (A,  $W_s$ ), pulse-off time (C,  $T_{off}$ ) and wire speed\*pulse-on time ( $A \times B$ ,  $W_s * T_{on}$ ) also have significant effects on kerf width. The effects of wire speed and pulse-off time on kerf width are quite close. No significant effect of other process parameters on kerf width was observed. When the F values and percentage contributions in Table 6 are taken into consideration, for  $K$ , the most effective parameters on  $R_z$  surface roughness were again the pulse-on time (B,  $T_{on}$ ) and wire speed (A,  $W_s$ ), with 43.29% and 16.06% percentage contributions, respectively. The most effective process parameters on  $R_t$  surface roughness were pulse-on time (B,  $T_{on}$ , 36.76%) and wire speed\*pulse-on time ( $A \times B$ ,  $W_s * T_{on}$ , 29.75%). Other process parameters did not have a significant effect on  $R_t$  (Table 7).

**Table 5. ANOVA results for  $K$**

Sources of variance	DoF	SS	MS	F Value	Percentage contribution
A	1	0.000288	0.000288	57.60	9.00
B	2	0.002414	0.001207	241.43	75.63
C	2	0.000292	0.000146	29.23	9.15
AxB	2	0.000139	0.000070	13.90	4.35
AxC	2	0.000019	0.000010	1.90	0.60
BxC	4	0.000019	0.000005	0.97	0.60
Residual Error	4	0.000020	0.000005		0.63
Total	17	0.003192			100.00

$R^2 = 99.3\%$   
 \*Significant at %95 confidence level. Tabulated F-ratio at %95 confidence level:  $F_{0.05;1;4}=7.71$

**Table 6. ANOVA results for  $R_z$**

Sources of variance	DoF	SS	MS	F Value	Percentage contribution
A	1	9.274	9.2737	12.91	16.06
B	2	25.000	12.5000	17.40	43.29
C	2	3.467	1.7334	2.41	6.00
AxB	2	8.017	4.0084	5.58	13.88
AxC	2	6.281	3.1403	4.37	10.88
BxC	4	2.833	0.7082	0.99	4.90
Residual Error	4	2.873	0.7183		4.98
Total	17	57.744			100

$R^2 = 71.6\%$   
 \*Significant at %95 confidence level. Tabulated F-ratio at %95 confidence level:  $F_{0.05;1;4}=7.71$

**Table 7. ANOVA results for  $R_t$**

Sources of variance	DoF	SS	MS	F Value	Percentage contribution
A	1	7.006	7.006	2.43	4.10
B	2	62.720	31.360	10.88	36.76
C	2	7.418	3.709	1.29	4.35
AxB	2	50.763	25.381	8.81	29.75
AxC	2	25.653	12.826	4.45	15.03
BxC	4	5.551	1.388	0.48	3.25
Residual Error	4	11.528	2.882		6.76
Total	17	170.638			100

$R^2 = 83.0\%$   
 \*Significant at %95 confidence level. Tabulated F-ratio at %95 confidence level:  $F_{0.05;1;4}=7.71$

#### 4.4. Predictive equations

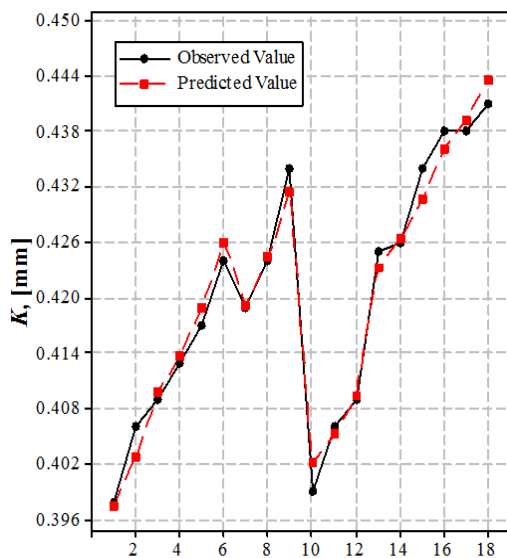
Many researchers (Saha et al., 2013, Manna A Bhattacharyya, 2006 and Sharma et al., 2013) have used first and second order predictive equations developed by using the regression technique. The second order predictive equations consisting of the effect of interactions of control factors on  $K$ ,  $R_z$  and  $R_t$  and quadratic effects are given in Equations 2-4. In these equations,  $Ws^2$  and  $T_{off}^2$  were neglected. The predictive equations are given below:

$$K = 0.308 - 0.000144Ws + 0.017T_{on} + 0.00343T_{off} + 0.000124WsT_{on} - 0.000035WsT_{off} + 0.000004T_{on}T_{off} - 0.00126T_{on}^2 \quad (2)$$

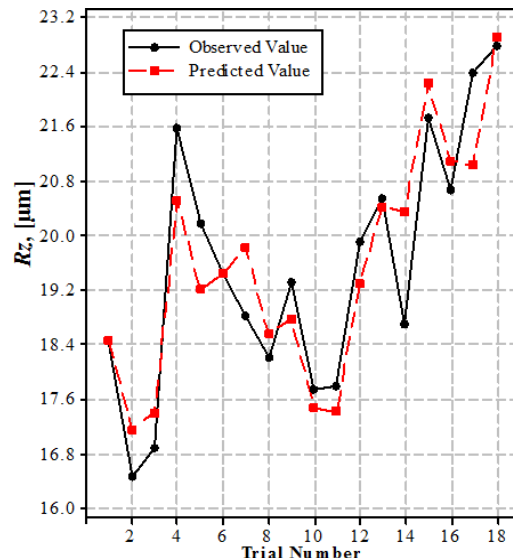
$$R_z = 27.8 - 0.304Ws + 2.91T_{on} - 2.66T_{off} + 0.0223WsT_{on} + 0.0206WsT_{off} + 0.0705T_{on}T_{off} - 0.250T_{on}^2 \quad (3)$$

$$R_t = 56.5 - 0.917Ws + 2.90T_{on} - 3.69T_{off} + 0.0767.WsT_{on} + 0.0403WsT_{off} + 0.0686T_{on}T_{off} - 0.451T_{on}^2 \quad (4)$$

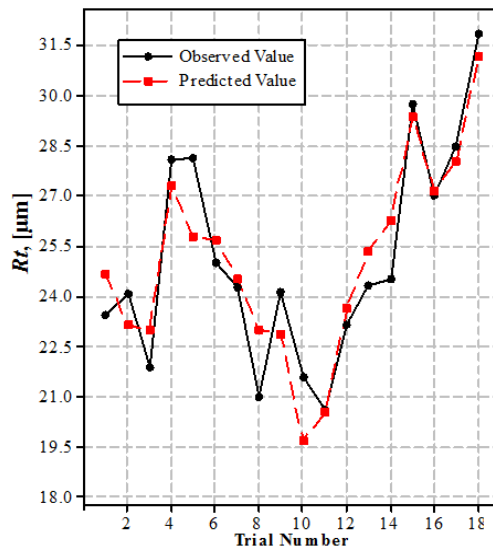
In Equation 2, the factors  $Ws$ ,  $WsToff$  and  $Ton2$  have a negative effect on  $K$ , while  $Ton$ ,  $Toff$ ,  $WsTon$  and  $TonToff$  have an additive impact on  $K$ . The predicted  $R^2$  (correlation coefficient) value (98.0%) and the adjusted  $R^2$  value (96.7%) matched with the experimental results. The adjusted  $R^2$  determines the amount of deviation about the mean, which is described by the model. In Equations 3 and 4, the factors  $Ws$ ,  $Toff$  and  $Ton2$  have a negative effect on  $R_z$ , while  $Ton$ ,  $WsTon$ ,  $WsToff$  and  $TonToff$  have an additive effect on  $R_z$  and  $R_t$ . The predicted  $R^2$  values (82.8% for  $R_z$  and 85.5% for  $R_t$ ) and the adjusted  $R^2$  values (70.7% for  $R_z$  and 75.4% for  $R_t$ ) were found to be in good agreement. The regression models were successfully adopted for estimating  $K$ ,  $R_z$  and  $R_t$ . The validation of the regression models developed for  $K$ ,  $R_z$  and  $R_t$  is given in Figures 7a-c. In Fig. 7a, the  $K$  values increased from Trials 1 to 9; the same increase can be observed again from Trials 9 to 18. In Trials 1 to 9, the  $Ws$  of 50 m/min remained constant, while the  $Ton$  increased from 5 to 10  $\mu s$  (Tables 1-2). This significant effect of  $Ton$  on  $K$  was also reflected in the predictive equation developed for  $K$ . As seen in Fig. 7b and 7c, especially in Trials 10-18,  $Ton$  had a similar effect on  $R_z$  and  $R_t$ . The  $R_z$  and  $R_t$  values increased with the increase of  $Ton$  from 5 to 10  $\mu s$  ( $Ws = 70$  m/min constant).



a)



b)



c)

**Figure 7:**

Comparison of observed (experimentally measured) and predicted values for a)  $K$ , b)  $R_z$  and c)  $R_t$ .

#### 4.5. Verification of experiments

For the determination of the validity of the optimum control factors in the TM, it was necessary to make verification tests. In the verification of optimum  $K$ ,  $R_z$  and  $R_t$  values, Equations 5-7 below were used.

$$K_{opt} = (A_1 - T_K) + (B_1 - T_K) + (C_1 - T_K) + T_K \tag{5}$$

$$Rz_{opt} = (A_1 - T_K) + (B_1 - T_K) + (C_2 - T_K) + T_{Rz} \tag{6}$$

$$Rt_{opt} = (A_1 - T_K) + (B_1 - T_K) + (C_2 - T_K) + T_{Rt} \tag{7}$$

In the above equations,  $(A_1, B_1, C_1)$ ,  $(A_1, B_1, C_2)$  and  $(A_1, B_1, C_2)$  are the respective optimum levels of  $K$ ,  $R_z$  and  $R_t$  (Table 2). The arithmetic means of the  $K$ ,  $R_z$  and  $R_t$  values obtained from the experimental study were  $T_K$ ,  $T_{Rz}$  and  $T_{Rt}$ , respectively. After calculation, it was determined that  $K_{opt} = 0.397$  mm,  $Rz_{opt} = 16.572$  µm and  $Rt_{opt} = 21.208$  µm. At this stage, verification of the optimized values had to be performed. Accepting the confidence level as 95%, Equation 8 was used in the calculation of the confidence interval (CI) for  $K_{opt}$ ,  $Rz_{opt}$  and  $Rt_{opt}$ .

$$CI_{K,Rz,Rt} = \sqrt{F_{\alpha,1,f_e} V_e \left[ \frac{1}{\eta_{eff}} + \frac{1}{R} \right]} \tag{8}$$

Here,  $\alpha$  is the necessary F ratio for the confidence interval,  $f_e$  is the error of degree of freedom (DoF),  $V_e$  is error of variance,  $\eta_{eff}$  is the effective number of replications and  $R$  is the number of replications for confirmation experiments. The  $\eta_{eff}$  was calculated by the aid of Equation 9.

$$\eta_{eff} = \frac{N}{1 + T_{dof}} \tag{9}$$

Here,  $N$  is the total number of tests and  $T_{dof}$  is the total degrees of freedom related to the average optimum;  $F_{0.05,1,4} = 7.71$  (from F test Table);  $V_{eK} = 0.000005$ ,  $V_{eRz} = 0.7183$  and  $V_{eRt} = 2.882$  (Table 5);  $R = 5$ ;  $N = 18$ ,  $T_{dof} = 13$  and  $\eta_{eff} = 1.286$  (Eq.9). The confidence intervals  $CI_K = 0.0061$ ,  $CI_{Rz} = 2.326$  and  $CI_{Rt} = 4.66$  were calculated by using Eqs. 8 and 9. At the 95% confidence level, the estimated average optimal  $K$  was calculated for  $R_z$  and  $R_t$  respectively as given below:

$$[K_{opt} - CI_K] < K_{opt} < [K_{opt} + CI_K] = [0.397 - 0.0061] < 0.397 < [0.397 + 0.0061] = 0.3909 < 0.397 < 0.4031$$

$$[Rz_{opt} - CI_{Rz}] < Rz_{opt} < [Rz_{opt} + CI_{Rz}] = [16.572 - 2.326] < 16.572 < [16.572 + 2.326] = 14.246 < 16.572 < 18.898$$

$$[Rt_{opt} - CI_{Rt}] < Rt_{opt} < [Rt_{opt} + CI_{Rt}] = [21.208 - 4.66] < 21.208 < [21.208 + 4.66] = 16.548 < 21.208 < 28.868$$

Therefore, the system optimization for  $K$ ,  $R_z$  and  $R_t$  was obtained by using the TM at the significance level of 0.05. Verification tests of the control factors were made for the TM (at the optimum and random levels) and for the developed regression equations. Table 8 gives the comparison of estimated values obtained by using the TM and linear regression equations (Eqs.2-4) and the test results and shows that the estimated values and test results were very close. The error values were lower than 10%, thus reflecting the reliability of the statistical analyses. The results of the verification tests also illustrate the success of the optimization process.

**Table 8. Predicted values and confirmation test results for  $K$ ,  $R_z$  and  $R_t$**

Level	For Taguchi method			For linear regression equations		
	Exp.	Pred.	Error (%)	Exp.	Pred.	Error (%)
<b><math>K</math> (mm)</b>						
$A_1, B_1, C_1$ (Optimum)	0.398	0.397	0.25	0.398	0.397	0.25
$A_1, B_2, C_3$ (Random)	0.424	0.425	0.24	0.424	0.425	0.24
<b><math>R_z</math> (<math>\mu\text{m}</math>)</b>						
$A_1, B_1, C_2$ (Optimum)	16.45	16.551	0.61	16.45	13.700	16.72
$A_2, B_3, C_1$ (Random)	20.68	20.634	0.22	20.68	22.639	9.47
<b><math>R_t</math> (<math>\mu\text{m}</math>)</b>						
$A_1, B_1, C_2$ (Optimum)	24.05	23.556	2.05	24.05	19.730	17.96
$A_2, B_1, C_2$ (Random)	20.60	21.094	2.40	20.60	17.120	16.90

## 5. CONCLUSION

In the cutting of Al/B<sub>4</sub>C-Gr composites by WEDM, the effects of the control factors on kerf and on  $R_z$  and  $R_t$  surface roughness were investigated. The following conclusions were obtained at the end of the study:

- According to ANOVA results, the most effective parameter on kerf, and on  $R_z$  and  $R_t$  surface roughness was pulse-on time, with contribution ratios of 75.63%, 43.29% and 36.76%, respectively. Other effective parameters for kerf were pulse-off time and wire speed, with respective contribution ratios of 9.15% and 9%.
- The effective parameters for  $R_z$  surface roughness were wire speed and pulse-off time, with contribution factors of 16.06% and 6%, respectively.
- The effective parameters for  $R_t$  surface roughness were wire speed and pulse-off time, with contribution ratios of 4.1% and 4.35%. However, significant effects of wire speed/pulse-on

time and wire speed/pulse-off time factor interactions were determined with respective contributions of 29.75% and 15.03%.

- While the  $R_z$  and  $R_t$  surface roughness increased depending on the wire speed increase, the same tendency was not observed for pulse-on time and pulse-off time.
- The optimum levels of the control factors were:  $A_1$  ( $Ws = 50\text{m/min}$ ),  $B_1$  ( $T_{on} = 5\mu\text{s}$ ) and  $C_1$  ( $T_{off} = 7\mu\text{s}$ ) for kerf ( $A_1B_1C_1$ ) and  $A_1$  ( $Ws = 50\text{m/min}$ ),  $B_1$  ( $T_{on} = 5\mu\text{s}$ ) and  $C_2$  ( $T_{off} = 10\mu\text{s}$ ) for  $R_z$  and  $R_t$  ( $A_1B_1C_2$ ). Kerf values increased depending on the increase of the overall control factors.
- The correlation coefficient ( $R^2$ ) of the predictive equations developed for the estimation of minimum kerf, and  $R_z$  and  $R_t$  surface roughness by linear regression analysis was calculated as 0.98, 0.828 and 0.855, respectively. The high correlation coefficients reflect the reliability of the developed equations.
- The error ratios of the estimated results obtained by the Taguchi method and predictive equations were less than 10% and indicated the reliability of the statistical analyses.

## REFERENCES

1. Ciftci İ, Turker M, Seker U. (2004) Evaluation of Tool Wear when Machining SiCp-Reinforced Al-2014 Alloy Matrix Composites, *Materials and Design*, 25, 251–255. doi:10.1016/j.matdes.2003.09.019
2. Durairaja M, Sudharsun D, Swamynathan N. (2013) Analysis of Process Parameters in Wire EDM with Stainless Steel Using Single Objective Taguchi Method and Multi Objective Grey Relational Grade, *Procedia Engineering*, 64, 868–877. doi:10.1016/j.proeng.2013.09.163
3. Fard RK, Afza RA, Teimouri R. (2013) Experimental Investigation, Intelligent Modeling and Multi-Characteristics Optimization of Dry WEDM Process of Al–SiC Metal Matrix Composite, *Journal of Manufacturing Processes*, 15, 483–494. doi:10.1016/j.jmapro.2013.09.002
4. Garg RK, Singh KK, Sachdeva A, Sharma VS, Ojha K, Singh S. (2010) Review of Research Work in Sinking EDM and WEDM on Metal Matrix Composite Materials, *International Journal of Advanced Manufacturing Technology*, 50, 611–624. doi:10.1007/s00170-010-2534-5
5. Hu HM, Lavernia EJ, Harrigan WC, Kajuch J, Nutt SR. (2001) Microstructural Investigation on  $B_4C/Al-7093$  Composite, *Materials Science and Engineering: A*, 297, 94–104. doi:10.1016/S0921-5093(00)01254-5
6. Iwai Y, Honda T, Miyajima T, Iwasaki Y, Surappa MK, Xu JF. (2000) Dry Sliding Wear Behavior of  $Al_2O_3$  Fiber Reinforced Aluminum Composites, *Composites Science and Technology*, 60, 1781–1789. doi:10.1016/S0266-3538(00)00068-3
7. Kevin Chou YR and Liu J. (2005) CVD Diamond Tool Performance in Metal Matrix Composite Machining, *Surface and Coatings Technology*, 200, 1872–1878. doi:10.1016/j.surfcoat.2005.08.094
8. Krishnamurthy L, Sridhara BK, Budan DA. (2007) Comparative Study on the Machinability Aspects of Aluminum Silicon Carbide and Aluminum Graphite Composites, *Materials and Manufacturing Processes*, 22, 903–908. doi:10.1080/10426910701451754

9. Lahane SD, Rodge MK, Sharma SB. (2012) Multi-response Optimization of Wire-EDM Process using Principal Component Analysis, *IOSR Journal of Engineering (IOSRJEN)*, 2, 38–47.
10. Lau WS, Yue TM, Lee TC, Lee WB. (1995) Un-conventional Machining of Composite Materials, *Journal of Materials Processing Technology*, 48, 199–205. doi:10.1016/0924-0136(94)01650-P
11. Lauwers B, Brans K, Liu W, Vleugels J, Salehi S, Vanmeensel K. (2008) Influence of the Type and Grain Size of the Electro-Conductive Phase on the Wire-EDM Performance of ZrO<sub>2</sub> Ceramic Composites, *CIRP Annals - Manufacturing Technology*, 57, 191–194. doi:10.1016/j.cirp.2008.03.089
12. Lin Q, Shen P, Qiu, F. Zhang D, Jiang Q. (2009) Wetting of Polycrystalline B<sub>4</sub>C by Molten Al at 1173–1473K, *Scripta Materialia*, 60, 960–963. doi: 10.1016/j.scriptamat.2009.02.024
13. Manna A Bhattacharyya B. (2006) Taguchi and Gauss Elimination Method: A Dual Response Approach for Parametric Optimization of CNC Wire Cut EDM of PRAISiC MMC, *Journal of Advanced Manufacturing Technology*, 28, 67–75. doi: 10.1007/s00170-004-2331-0
14. Montgomery DC. (1991) *Taguchi's Contributions to Experimental Design and Quality Engineering, Design and Analysis of Experiment*; John Wiley and Sons, Canada.
15. Muthuraman V, Ramakrishnan R. (2012) Multi Parametric Optimization of WC-Co Composites Using Desirability Approach, *Procedia Engineering*, 38, 3381–3390. doi:10.1016/j.proeng.2012.06.391
16. Patil NG, Brahmkankar PK. (2010) Determination of Material Removal Rate in Wire Electro-Discharge Machining of Metal Matrix Composites using Dimensional Analysis, *Journal of Advanced Manufacturing Technology*, 51, 599–610.
17. Patil NG, Brahmkankar PK. (2010) Some Studies into Wire Electro-Discharge Machining of Alumina Particulate-Reinforced Aluminum Matrix Composites, *Journal of Advanced Manufacturing Technology*, 48, 537–555. doi: 10.1007/s00170-009-2291-5
18. Praskash JU, Moorthy TV, Peter JM. (2013) Experimental Investigation on Machinability of Aluminium Alloy (A413)/Flyash/B<sub>4</sub>C Hybrid Composites Using Wire EDM, *Procedia Engineering*, 64, 1344–1353. doi: 10.1016/j.proeng.2013.09.216
19. Puhan D, Mahapatra SS, Sahu J, Das L. (2013) A Hybrid Approach for Multi-Response Optimization of Non-Conventional Machining on AlSiCp MMC, *Measurement*, 46, 3581–3592. doi: 10.1016/j.measurement.2013.06.007
20. Ravikiran A, Surappa MK. (1997) Effect of Sliding Speed on Wear Behavior of A356 Al 30 wt % SiCp MMC, *Wear*, 206, 33–38. doi:10.1016/S0043-1648(96)07341-3
21. Ross PJ. (1996) *Taguchi Techniques for Quality Engineering. Loss Function, Orthogonal Experiments Parameter and Tolerance Design*, McGraw-Hill, New York.
22. Rozenek M, Kozak J, Dabrowski L, Lubkowski K. (2001) Electrical Discharge Machining Characteristics of Metal Matrix Composites, *Journal of Materials Processing Technology*, 109, 367–370. doi:10.1016/S0924-0136(00)00823-2
23. Rubio JCC, Silva LJ, Leite WO, Panzera TH, Filho SLMR, Davim JP. (2013) Investigations on the Drilling Process of Unreinforced and Reinforced Polyamides using Taguchi Method, *Composite Part B*, 55, 338–344. doi: 10.1016/j.compositesb.2013.06.042

24. Saha P, Singha A, Pal SK, Saha P. (2008) Soft Computing Models Based Prediction of Cutting Speed and Surface Roughness in Wire Electro-Discharge Machining of Tungsten Carbide Cobalt Composite, *Journal of Advanced Manufacturing Technology*, 39, 74–84. doi: 10.1007/s00170-007-1200-z
25. Saha P, Tarafdar D, Pal SK, Saha P, Srivastava AK, Das K. (2013) Multi-Objective Optimization in Wire-Electro-Discharge Machining of TiC Reinforced Composite through Neuro-Genetic Technique, *Applied Soft Computing*, 13, 2065–2074. doi:10.1016/j.asoc.2012.11.008
26. Satishkumar D, Kanthababu, M, Vajjiravelu V, Anburaj R, Sundarrajan NT, Arul H. (2011) Investigation of Wire Electrical Discharge Machining Characteristics of Al6063/SiCp Composites, *Journal of Advanced Manufacturing Technology*, 56, 975–986. doi: 10.1007/s00170-011-3242-5
27. Shandilya P, Jain PK, Jain NK. RSM and ANN Modeling Approaches for Predicting Average Cutting Speed during WEDM of SiCp/6061 Al MMC, *Procedia Engineering*, 64, 767–774. doi:10.1016/j.proeng.2013.09.152
28. Sharma N, Khanna R, Gupta R. (2013) Multi Quality Characteristics of WEDM Process Parameters with RSM, *Procedia Engineering*, 64, 710–719. doi: 10.1016/j.proeng.2013.09.146
29. Singh H, Garg R. (2009) Effects of Process Parameters on Material Removal Rate in WEDM, *Journal of of Achievements in Materials and Manufacturing Engineering*, 32, 70–74.
30. Tosun N, Cogun C, Tosun G. (2004) A Study on Kerf and Material Removal Rate in Wire Electrical Discharge Machining Based on Taguchi Method, *Journal of Materials Processing Technology*, 152, 316–322. doi:10.1016/j.jmatprotec.2004.04.373
31. Vankanti VK, Ganta V. (2014) Optimization of Process Parameters in Drilling of GFRP Composite using Taguchi Method, *Journal of Materials Research and Technology*, 3, 35–41. doi:10.1016/j.jmrt.2013.10.007
32. Yan BH, Tsai HC, Huang FY, Lee LC. (2005) Examination of Wire Electrical Discharge Machining of Al<sub>2</sub>O<sub>3</sub>p/6061Al Composites, *International Journal of Machine Tools and Manufacture*, 45, 251–259. doi: 10.1016/j.ijmachtools.2004.08.015





